Cell Reports
Report

# miR-342-5p Decreases Ankyrin G Levels in Alzheimer's Disease Transgenic Mouse Models

Xiaqin Sun,[1] Yu Wu,[1] Mingxue Gu,[1] and Yan Zhang[1,*]
[1]State Key Laboratory of Biomembrane and Membrane Biotechnology, College of Life Sciences, PKU-IDG/McGovern Institute for Brain Research, Peking University, Beijing 100871, China
*Correspondence: yanzhang@pku.edu.cn
http://dx.doi.org/10.1016/j.celrep.2013.12.028


## SUMMARY

**MicroRNA alterations and axonopathy have been reported in patients with Alzheimer's disease (AD) and in AD mouse models. We now report that miR-342-5p is upregulated in APP/PS1, PS1ΔE9, and PS1-M146V transgenic AD mice, and that this upregulation is mechanistically linked to elevated β-catenin, c-Myc, and interferon regulatory factor-9. The increased miR-342-5p downregulates the expression of ankyrin G (AnkG), a protein that is known to play a critical role at the axon initial segment. Thus, a specific miRNA alteration may contribute to AD axonopathy by downregulating AnkG.**

## INTRODUCTION

MicroRNAs (miRNAs) are a class of short (usually 21–23 nt) noncoding RNAs (Lagos-Quintana et al., 2001) with conserved roles in *Drosophila*, rodents, monkeys, and humans (Ashraf et al., 2006; Elmén et al., 2008; Hollander et al., 2010; Jin et al., 2004); in mammals, over 1,000 miRNAs have been identified (Delay et al., 2012). miRNA precursors are first processed into a single-stranded miRNA that interacts with the 3′ UTR of the complementary mRNA sequences (Peters and Meister, 2007), resulting in translation repression or target degradation (Eulalio et al., 2009; Meister, 2007). A single miRNA can have up to several hundred target genes and thus may regulate multiple pathways at the same time (Baek et al., 2008; Selbach et al., 2008). Many miRNAs have demonstrated implications in neurodegenerative diseases, such as Alzheimer's disease (AD) (Chan and Kocerha, 2012; Delay and Hébert, 2011; Delay et al., 2012), which is the most common cause of dementia in people over 65 years of age and is associated with impairments in memory, language, behavior, and cognition (Price et al., 1995).

The brains of patients with AD are characterized by the presence of senile plaques and neurofibrillary tangles (Price et al., 1995), together with axonal pathology involving dystrophic neurites decorating amyloid plaques, axonal swellings, and abnormal accumulation of axonal proteins (Bayer et al., 2001). Axonopathy and axonal transport deficits have been found in other neurodegenerative diseases as well (Roy et al., 2005; Yagishita, 1978). In this regard, abundant age-dependent axonal spheroids and myelin ovoids have been observed in the spinal cord of APP/PS1 mice, an established AD transgenic mouse model (Wirths et al., 2006). However, the cause of the axonopathy and the pathways involved in axonal abnormalities in AD remain largely unknown. The axon initial segment (AIS) is known to play an important role in neuronal polarity formation, action potential initiation (Rasband, 2010; Szu-Yu Ho and Rasband, 2011), and brain diseases and injury (Buffington and Rasband, 2011). Ankyrin G (AnkG) has been demonstrated to play an important role in maintaining the structure of AIS and in the generation/maintenance of neuronal polarity (Hedstrom et al., 2008; Kapfhamer et al., 1995; Kordeli et al., 1995; Sobotzik et al., 2009). AnkG was found to link membrane proteins to the cytoskeleton and play critical roles in the stabilization of membrane domains (Bennett and Chen, 2001) and neuronal polarity (Sobotzik et al., 2009). Neuronal injury could result in the loss of AnkG (Schafer et al., 2009). At the AIS, the critical function of AnkG has been reported to mediate sodium channel localization (Pan et al., 2006) and the establishment of selective filtering machinery (Song et al., 2009).

In the present study, we report that in APP/PS1, PS1ΔE9, and PS1-M146V mouse hippocampal neurons, miR-342-5p, a miRNA that targets AnkG mRNA 3′ UTR, is highly upregulated compared with wild-type (WT) mouse neurons. Furthermore, we show that downregulation of AnkG by miR-342-5p is mediated through translation repression. Our results point to miRNA regulation as a critical determinant of axonal and neuronal pathology in AD mouse models.

## RESULTS

### Upregulation of miR-342-5p in the Hippocampus of AD Transgenic Mice

Microarray analysis of miRNAs was performed on pooled hippocampal tissues from WT (n = 16) and APP/PS1 mice (n = 16) at embryonic day 14 (E14). Our data showed that, with the criterion of a 2-fold cutoff, seven miRNAs were upregulated (Figure 1A, red dots) and seven miRNAs were downregulated (green dots) in APP/PS1 hippocampal tissues as compared with WT hippocampal tissues. Among these altered miRNAs, miR-342-5p

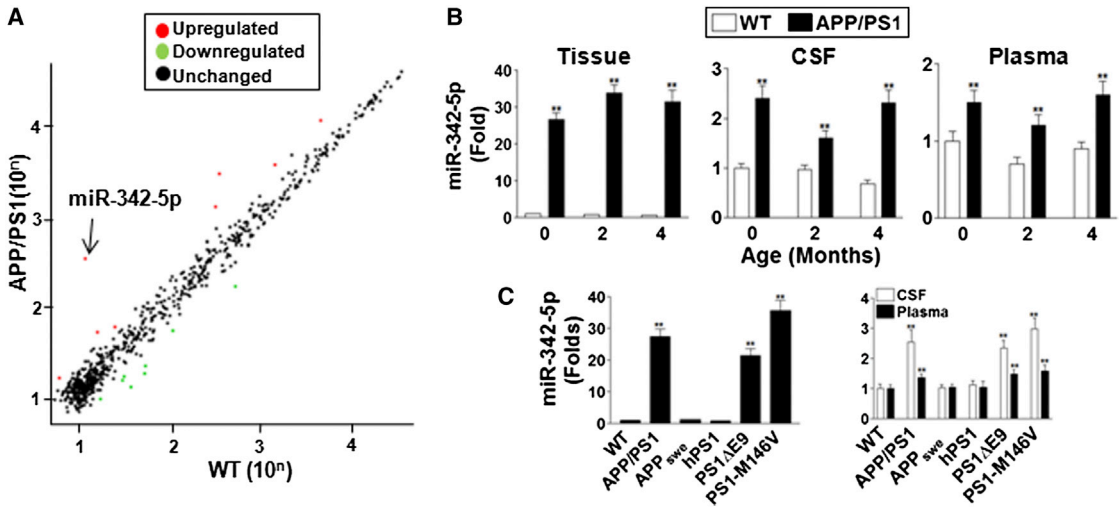


**Figure 1. miR-342-5p Was Upregulated in APP/PS1, PS1ΔE9, and PS1-M146V Mice**

(A) A miRNA array assay was done with hippocampal tissues from E14 WT (n = 16, pooled) and APP/PS1 (n = 16, pooled) mice. One of miRNAs that showed a significant increase in APP/PS1 mice was miR-342-5p.

(B) Left panel: miR-342-5p increased ~30-fold in the hippocampal tissues from APP/PS1 mice as compared with WT mice at 0, 2, and 4 months of age. Middle and right panels: miR-342-5p was secreted via an unknown mechanism and detected in the CSF and plasma. In CSF and plasma from APP/PS1 mice, miR-342-5p was upregulated at 0, 2, and 4 months of age compared with WT mouse samples.

(C) Left panel: increased miR-342-5p was found in E14 APP/PS1, PS1ΔE9, and PS1-M146V neurons, but not in APPswe or WT human PS1 (hPS1) transgenic mouse neurons, indicating that in PS1 a mutation contributed to the APP/PS1 phenotype upon miR-342-5p alteration. Right panel: miR-342-5p levels were significantly higher in the CSF and plasma of newborn APP/PS1, PS1ΔE9, and PS1-M146V mice, but not in APPswe or hPS1 mice. Data represent mean ± SE (n = 10 for each group). **p < 0.01 compared with controls.

was prominently increased and showed an ~22-fold upregulation in APP/PS1 hippocampus (Figure 1A). This upregulation was further verified by RT-PCR measurements of the miR-342-5p level in hippocampal tissues from WT and APP/PS1 mice at 0, 2, and 4 months of age (Figure 1B). Previous studies have shown that miRNAs can be secreted into the cerebrospinal fluid (CSF) and plasma (Chan and Kocerha, 2012). In this regard, we observed that miR-342-5p levels were elevated in the CSF and plasma of APP/PS1 samples compared with WT samples collected at 0, 2, and 4 months of age (Figure 1B).

Since APP/PS1 mice harbor transgenes encoding the familial AD (FAD)-linked APPswe and PS1ΔE9 polypeptides, we sought to examine changes in miR-342-5p in transgenic mice expressing the genes individually (APPswe, human WT PS1 [hWTPS1], or PS1ΔE9), together with an independent transgenic line expressing the FAD-linked PS1-M146V variant. Interestingly, we found that miR-342-5p was selectively upregulated in all PS1 mutant lines compared with the hWTPS1 and APPswe mutant lines (Figure 1C). The increase in the miR-342-5p level was confirmed in the CSF and plasma in the single-gene transgenic lines as well (Figure 1C).

## AnkG mRNA 3′ UTR Was a Target of miR-342-5p

Complementary sequences for miR-342-5p are present in the 3′ UTR of AnkG mRNA in both mouse and human (Figure S1A). In SH-SY5Y cells, luciferase reporter assays were performed with the expression of firefly regulated by the AnkG mRNA 3′ UTR complementary region to miR-342-5p, and renilla as an internal control for transfection efficiency. We found that miR-342-5p induced a dose-dependent inhibition of luciferase activity, whereas mutant miR-342-5p and scramble control (Scr) miRNA had no effect (Figure 2A). The mimic of miR-342-5p markedly inhibited the luciferase activity, whereas the inhibitor of miR-342-5p increased the luciferase activity (Figure 2A). A time-course study showed that miR-342-5p inhibited luciferase activity from 6 to 48 hr after treatment (Figure 2B). In SH-SY5Y cells, an enhanced GFP (EGFP) reporter assay confirmed that miR-342-5p had a similar inhibitory effect on AnkG mRNA 3′ UTR (Figures S1C and S1D).

We then mutated the AnkG mRNA 3′ UTR complementary sequence and performed luciferase assays with either Scr miRNA or miR-342-5p. Our results indicated that miR-342-5p suppressed the luciferase activity with WT AnkG mRNA 3′ UTR, but not with mutant 3′ UTR (Figures 2C and S1E), suggesting the specificity of the interaction between miR-342-5p and AnkG mRNA 3′ UTR. To further validate that the AnkG mRNA 3′ UTR was one of the targets for miR-342-5p, we made mutant AnkG mRNA 3′ UTR with two repeats of the putative complementary binding domain (BD) sequence (2BD) and three repeats of the BD sequence (3BD). The luciferase reporter system showed that miR-342-5p did not suppress the luciferase activity regulated by unrelated MAP2 mRNA 3′ UTR (Figure 2C). With AnkG mRNA 3′ UTR, luciferase activity was greatly reduced in a BD-dose-dependent manner (Figure 2C). To examine the specificity of miR-342-5p targeting AnkG mRNA, we tested all seven miRNAs upregulated in APP/PS1 tissues, as detected by microarray assay (Figure 1A),

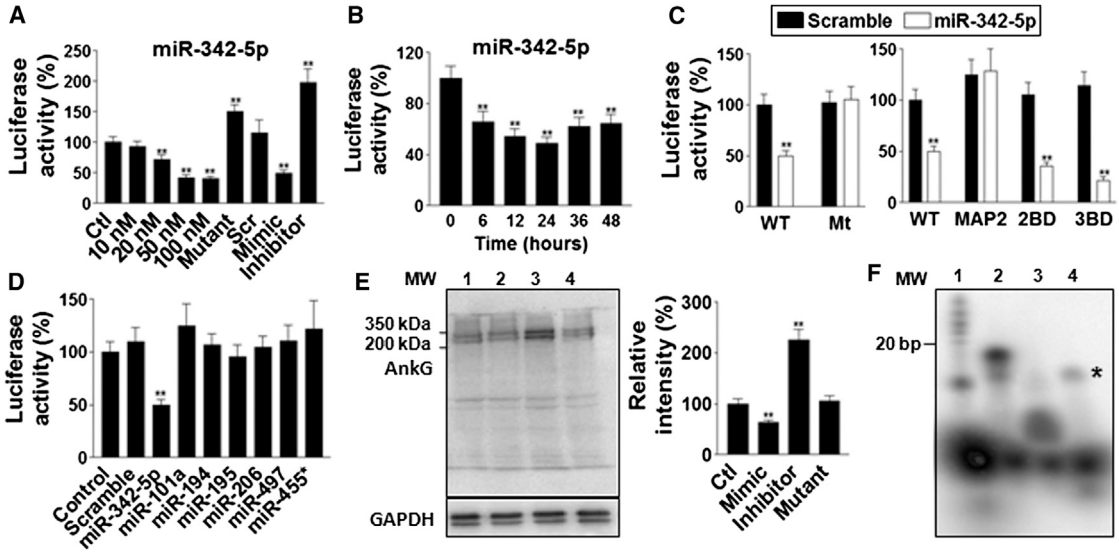


**Figure 2. miR-342-5p Regulated AnkG mRNA 3′ UTR and Decreased AnkG Expression**

(A) Dose response of miR-342-5p on luciferase reporter assay in SH-SY5Y cells.

(B) Time course of miR-342-5p inhibition on AnkG mRNA 3′ UTR.

(C) Left panel: miR-342-5p reduced the luciferase activity with WT AnkG mRNA 3′ UTR, but not with mutant AnkG mRNA 3′ UTR. Right panel: miR-342-5p did not alter the expression with unrelated MAP2 mRNA 3′ UTR. With AnkG mRNA 3′ UTR constructed with a 2- or 3-fold greater amount of the putative binding domain (2BD or 3BD), miR-342-5p decreased luciferase activity remarkably in a BD dose-dependent manner.

(D) Other miRNAs pulled out in the miRNA array assay were tested against luciferase activity driven by AnkG mRNA 3′ UTR. Only miR-342-5p specifically decreased luciferase activity. Data represent mean ± SE (n = 10 for each group). **p < 0.01 compared with controls.

(E) Western blot of AnkG, using the antibody provided by Dr. V. Bennett (Duke University), shows that the mimic of miR-342-5p (lane 2) reduced the AnkG levels, whereas the inhibitor of miR-342-5p (lane 3) increased them. Mutant miR-342-5p (lane 4) did not alter the AnkG levels. Data represent mean ± SE (n = 3 for each group). **p < 0.01 compared with control.

(F) The RNase protection assay shows that in the mixture of AnkG mRNA 3′ UTR with miR-342-5p (lane 4), the negative control antisense reversed sequence (miR-342-5p, lane 3) and the positive control synthesized complementary sequence (miR-342-5p, lane 2) effectively protected AnkG mRNA 3′ UTR from RNase digestion (*), suggesting direct binding of miR-342-5p with AnkG mRNA 3′ UTR. Lane 1: molecular weight marker.

against luciferase reporter activity regulated by AnkG mRNA 3′ UTR. Only miR-342-5p effectively inhibited luciferase activity (Figure 2D).

When different concentrations of miR-342-5p were transfected into SH-SY5Y cells, measurements of AnkG mRNA levels in various concentrations of miR-342-5p, the mimic of miR-342-5p (M-miR-342-5p), and the inhibitor of miR-342-5p (I-miR-342-5p) showed no difference (Figure S1B), suggesting that miR-342-5p likely modulates AnkG levels through translation repression rather than mRNA degradation. Western blotting of AnkG with the mimic of miR-342-5p, inhibitor of miR-342-5p, and mutant miR-342-5p indicated that miR-342-5p indeed decreased AnkG levels (Figure 2E). Direct binding of miR-342-5p and AnkG mRNA 3′ UTR was demonstrated by RNase protection assay. A synthesized miR-342-5p sequence (lane 4) and its antisense reversed sequence (lane 3) were labeled with $^{32}$P probe and mixed with AnkG mRNA 3′ UTR. After RNase digestion, single-stranded RNAs were degraded, whereas bonded, double-stranded RNAs remained. Compared with the positive control (lane 2), where the exact complementary sequence to miR-342-5p was used, miR-342-5p (lane 4) showed a clear band (*), suggesting its direct binding to AnkG mRNA 3′ UTR (Figure 2F).

## Downregulation of AnkG in AD Transgenic Mice

Using immunostaining of AnkG, we found that AnkG was expressed in the axon and highly localized to the AIS in 7 days in vitro (DIV) WT mouse neurons, whereas the AnkG level was much lower in APP/PS1 mouse neurons, although localized AnkG distribution in the AIS remained detectable (Figure 3A). Western blot data from single-gene transgenic lines indicated that in PS1 mutated lines, AnkG levels were markedly reduced (Figure 3B), whereas mRNA levels of AnkG remained unchanged in various lines (Figure 3F). Western blots further showed that APP/PS1 mouse neurons had up to a 60% reduction of the total AnkG level in APP/PS1 mouse neurons at 2, 3, and 5 DIV as compared with WT neurons (Figures 3C and 3D). This reduction was found by using AnkG antibodies from two different sources (Figure S2A). In adult mice at age of 2, 6, and 8 months, APP/PS1 mouse hippocampal tissues had lower levels of AnkG compared with WT tissues (Figures 3C and 3E).

The levels of AnkG mRNA were examined in WT and APP/PS1 mice hippocampal tissues at different ages (Figure S2B). Interestingly, although the protein levels of AnkG in APP/PS1 mice were lower than in WT mice, the mRNA levels did not show significant differences between WT and APP/PS1 mice (Figure S2B), suggesting that the downregulation of AnkG in APP/PS1 mice

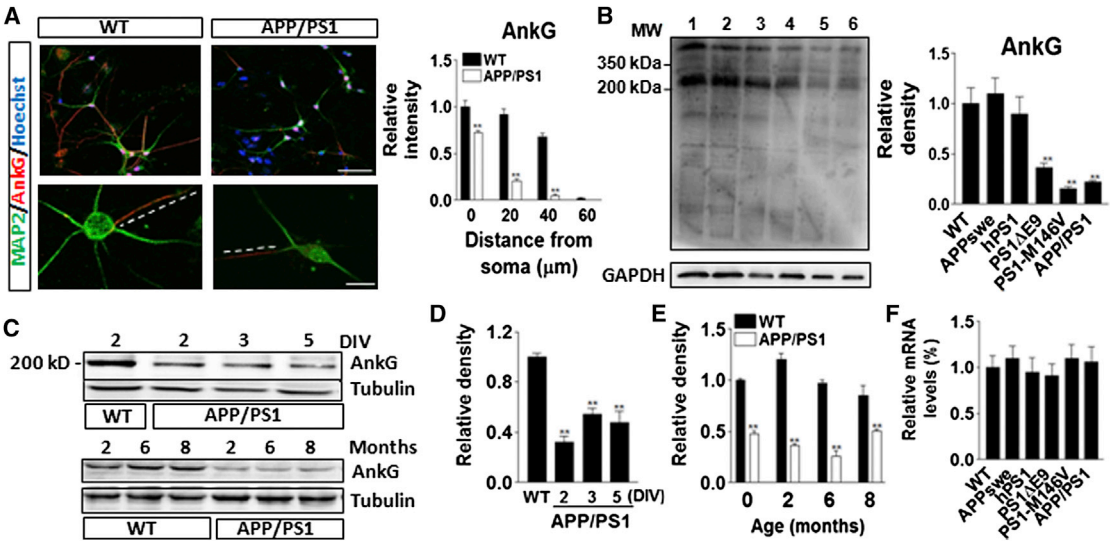


**Figure 3. AnkG Was Downregulated in APP/PS1, PS1ΔE9, and PS1-M146V Mouse Neurons**

(A) Left panel: at 7 DIV, AnkG distributed in the axon in WT mouse neurons, but only slightly in the axon in APP/PS1 mouse neurons. Scale bars, 50 μm (upper panels) and 10 μm (lower panels). Dashed line, AIS. Right panel: quantification of relative AnkG intensity in WT and APP/PS1 neurons.

(B) AnkG decreased in PS1ΔE9, PS1-M146V, and APP/PS1 neurons, but not in APPswe or hPS1 neurons. Lane 1: WT; lane 2: APPswe; lane 3: hPS1; lane 4: PS1ΔE9; lane 5: PS1-M146V; lane 6: APP/PS1.

(C–E) Western blots (with Invitrogen antibody) show that in neuronal culture at 2, 3, and 5 DIV of E14 embryos and in hippocampal tissues at 0, 2, 6, and 8 months of age, APP/PS1 mouse neurons and tissues had a smaller amount of AnkG as compared with WT.

(F) The mRNA levels in APPswe, hPS1, PS1ΔE9, PS1-M146V, and APP/PS1 neurons were not significantly different. Data represent mean ± SE (n = 10 for each group). **p < 0.01 compared with WT.

was due to either accelerated degradation or reduced protein expression at the translation level.

## DISCUSSION

In the present study, we find that miR-342-5p is upregulated in AD transgenic mice, including APP/PS1, PS1ΔE9, and PS1-M146V lines. Furthermore, miR-342-5p binds directly to the 3′ UTR of AnkG mRNA and decreases AnkG levels through translation repression in AD transgenic mouse neurons. miRNA profiling has been studied in the brain, blood, and CSF of Parkinson's disease patients (Cogswell et al., 2008; Hébert et al., 2008; Lukiw, 2007, Lukiw et al., 2008; Nelson and Wang, 2010; Nunez-Iglesias et al., 2010; Schipper et al., 2007; Shioya et al., 2010; Wang et al., 2008) and mouse models (Krichevsky et al., 2003; Li et al., 2011; Wang et al., 2009; Yao et al., 2010). Using APPswe/PS1ΔE9 mouse cortical tissues at 3 and 6 months of age, Wang et al. (2009) reported 37 differentially expressed miRNAs, which did not include miR-342-5p (Wang et al., 2009). The tissue specificity may account for this discrepancy, since we used hippocampal tissues in this study.

Our data show that PS1 mutation resulted in the most significant miR-342-5p upregulation. miR-342-5p is produced by "dicing" its parental miRNA, miR-342 (Westholm and Lai, 2011). To investigate how PS1 mutants increase miR-342-5p levels, we first examined the parent miR-342 levels in the hippocampal tissues from different mouse lines. Our data indicated that PS1 mutant lines express elevated miR-342 levels (Figure 4A), suggesting that PS1 mutants might regulate miR-342 at the transcriptional level. In vitro studies have revealed that expression of either PS1ΔE9 or PS1-M146V variants can increase β-catenin levels (Soriano et al., 2001), and indeed, we also observed a similar upregulation of β-catenin in embryonic hippocampal tissues from APP/PS1, PS1ΔE9, and PS1-M146V mice (Figure 4B). A transcriptional target of β-catenin is c-Myc (Smalley and Dale, 1999), and we now show that elevated β-catenin expression leads to increased c-Myc levels, which in turn elevate the levels of interferon regulatory factor 9 (IRF-9), as expected (Figure 4B; Seitz et al., 2011). miR-342 is localized in the intron Enah/Vasp-like (EVL) gene (Grady et al., 2008), and it is known that one of the critical transcription factors that activate the EVL promoter is IRF-9 (De Marchis et al., 2009). Hence, we would suggest that elevated IRF-9 leads to an increase in miR-342 levels. Taken together, our studies indicate that PS1ΔE9 and PS1-M146V mutants increased miR-342-5p levels through upregulation of β-catenin, c-Myc, and IRF-9. As the parent miRNA to miR-342-5p, miR-342 is diced into miR-342-5p and miR-342-3p (Westholm and Lai, 2011). Given that miR-342 and miR-342-5p are increased, it is not known why an increase in another strand, miR-342-3p, is not observed. Probably miR-342-3p does not successfully bind to the targets as miR-342-5p does, and then is degraded rapidly.

AnkG has been associated with AIS filtering and protein trafficking (Song et al., 2009). In APP/PS1 mice, axonopathy has been described as age-dependent axonal spheroids and myelin ovoids in the spinal cord (Wirths et al., 2006). In PS1 mutant mice (PS1ΔE9 and PS1-M146V), impaired fast axonal transport has been demonstrated (Lazarov et al., 2007). It is possible that in

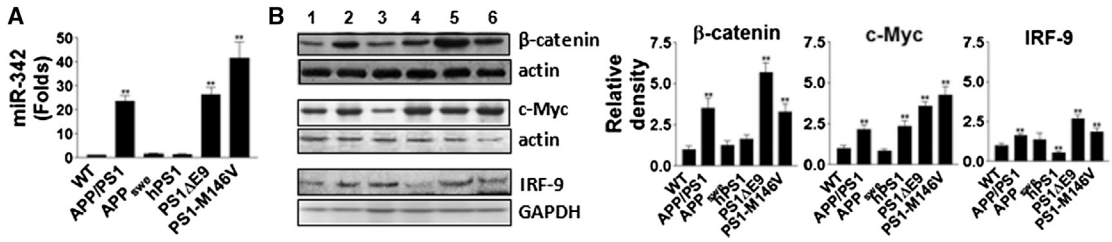


**Figure 4. PS1 Regulated miR-342-5p Levels through β-catenin, c-Myc, and IRF-9**

(A) RT-PCR of miR-342 levels in hippocampal tissues from E14 mice of different lines.

(B) Western blots of β-catenin, c-Myc, and IRF-9 in hippocampal tissues from E14 mice of different lines. Lane 1: WT; lane 2: APP/PS1; lane 3: APPswe; lane 4: hPS1; lane 5: PS1ΔE9; lane 6: PS1-M146V. Data represent mean ± SE (n = 3 for each group). **p < 0.01 compared with controls.

APP/PS1 and PS1 mutant mice, due to downregulation of AnkG by miR-342-5p, the AIS filtering is impaired, resulting in abnormal trafficking of proteins. The defective protein trafficking may induce protein aggregation in the axon, leading to impaired axonal fast transport. This may contribute to the axonopathy observed in AD and other neurodegenerative diseases. Finally, AD has been considered to be an aging-related disorder. Our data show that developmental defects in miRNA regulation, AIS filtering, and protein trafficking and localization could be involved in AD pathogenesis.

## EXPERIMENTAL PROCEDURES

### Cell Culture, Microinjection, and Treatments

Primary neurons were cultured from E14 APP/PS1 (APPswe/PS1ΔE9), APPswe, WT human PS1 knockin (hPS1), PS1ΔE9, and PS1-M146V mice hippocampus, following the regulations of the Peking University Animal Care and Use Committee as previously described (Cui et al., 2011). SH-SY5Y cells were cultured with minimum essential medium (Invitrogen).

miRNA levels were measured by the CapitalBio (Beijing, China) microarray service using GeneChip miRNA 2.0 (Affymetrix). miR-342-5p in the serum and CSF was measured with the TaqMan MicroRNA assay kit (Life Technologies) for Mmu-miR-342-5p according to the manufacturer's instructions. All miRNAs were transfected into SH-SY5Y cells with HiPerFect Transfection Agent (QIAGEN).

### RNase Protection Assay

To make the probe, we replaced the 5′ end phosphate group of human miR-342-5p and its reversed control strands with $^{32}$P (neg502a001MC; PerkinElmer) by T4 Polynucleotide Kinase (M0201S; PerkinElmer). The complementary sequence and human AnkG 3′ UTR mRNA (5′-TTGATAAGGCAC TGCCTCTTAGAACA-3′) were synthesized and purchased from QIAGEN. The $^{32}$P-labeled miR-342-5p, its reversed control or complementary sequence, and AnkG mRNA 3′ UTR were added in the hybridization buffer at 80°C for 2 min, and then incubated at 45°C for 18 hr. RNase A (D202; Takara) was added to the sample at 37°C for 30 min. The RNAs were purified and run into 15% PAGE. The gel was dried and revealed by autoradiography.

### Immunostaining

Cells were permeabilized in PBS-Triton at 4°C, blocked in 10% donkey serum at room temperature, and then incubated with AnkG antibody (4G3F8, Invitrogen, 1:200) or MAP2 (Abcam) at 4°C for 24 hr. Cy2- or Cy3-conjugated donkey anti-rabbit antibodies and AMCA-conjugated goat anti-chicken antibody were applied as the secondary antibodies. The nuclei were stained with Hoechst 33258 (1 μg/ml; Sigma) for 15 min in the dark. The coverslips were mounted with Immunon mounting medium (Shandon) onto glass slides and the results were analyzed with the use of laser confocal fluorescence microscope (Leica TCS SP5). A Super Resolution N-SIM Microscope (Nikon) was used to analyze high-resolution data. The average fluorescence intensities were measured at various distances from the soma area using NIS-Ements AR software (Nikon). To quantify the data, 15 frames were averaged with subtraction of background fluorescence intensity.

## ACCESSION NUMBERS

The microarray data reported in this paper has been deposited in the NCBI Gene Expression Omnibus under accession number GSE53859.

## SUPPLEMENTAL INFORMATION

Supplemental Information includes Supplemental Experimental Procedures and two figures and can be found with this article online at http://dx.doi.org/10.1016/j.celrep.2013.12.028.

## AUTHOR CONTRIBUTIONS

X.S., Y.W., and M.G. performed all of the experiments and analyzed the data. Y.Z. conceptualized the study, performed analyses, and drafted the manuscript.

## ACKNOWLEDGMENTS

The authors thank Dr. Sangram Sisodia (University of Chicago) and Dr. Vann Bennett (Duke University) for their inspiring thoughts and helpful suggestions regarding the project and the manuscript. Dr. Sisodia also provided all of the PS1 mutant mouse lines and Dr. Bennett provided the AnkG antibody. This work was supported by the National Science Foundation of China (NSFC; Major Research Grant 91132718).

Received: May 27, 2013
Revised: September 22, 2013
Accepted: December 17, 2013
Published: January 16, 2014

## REFERENCES

Ashraf, S.I., McLoon, A.L., Sclarsic, S.M., and Kunes, S. (2006). Synaptic protein synthesis associated with memory is regulated by the RISC pathway in Drosophila. Cell *124*, 191–205.

Baek, D., Villén, J., Shin, C., Camargo, F.D., Gygi, S.P., and Bartel, D.P. (2008). The impact of microRNAs on protein output. Nature *455*, 64–71.

Bayer, T.A., Wirths, O., Majtényi, K., Hartmann, T., Multhaup, G., Beyreuther, K., and Czech, C. (2001). Key factors in Alzheimer's disease: beta-amyloid precursor protein processing, metabolism and intraneuronal transport. Brain Pathol. *11*, 1–11.

Bennett, V., and Chen, L. (2001). Ankyrins and cellular targeting of diverse membrane proteins to physiological sites. Curr. Opin. Cell Biol. *13*, 61–67.

Buffington, S.A., and Rasband, M.N. (2011). The axon initial segment in nervous system disease and injury. Eur. J. Neurosci. *34*, 1609–1619.

Chan, A.W., and Kocerha, J. (2012). The path to microRNA therapeutics in psychiatric and neurodegenerative disorders. Front Genet *3*, 82.

Cogswell, J.P., Ward, J., Taylor, I.A., Waters, M., Shi, Y., Cannon, B., Kelnar, K., Kemppainen, J., Brown, D., Chen, C., et al. (2008). Identification of miRNA changes in Alzheimer's disease brain and CSF yields putative biomarkers and insights into disease pathways. J. Alzheimers Dis. *14*, 27–41.

Cui, J., Wang, Y., Dong, Q., Wu, S., Xiao, X., Hu, J., Chai, Z., and Zhang, Y. (2011). Morphine protects against intracellular amyloid toxicity by inducing estradiol release and upregulation of Hsp70. J. Neurosci. *31*, 16227–16240.

De Marchis, M.L., Ballarino, M., Salvatori, B., Puzzolo, M.C., Bozzoni, I., and Fatica, A. (2009). A new molecular network comprising PU.1, interferon regulatory factor proteins and miR-342 stimulates ATRA-mediated granulocytic differentiation of acute promyelocytic leukemia cells. Leukemia *23*, 856–862.

Delay, C., and Hébert, S.S. (2011). MicroRNAs and Alzheimer's disease mouse models: current insights and future research avenues. Int. J. Alzheimers Dis. *2011*, 894938.

Delay, C., Mandemakers, W., and Hébert, S.S. (2012). MicroRNAs in Alzheimer's disease. Neurobiol. Dis. *46*, 285–290.

Elmén, J., Lindow, M., Schütz, S., Lawrence, M., Petri, A., Obad, S., Lindholm, M., Hedtjärn, M., Hansen, H.F., Berger, U., et al. (2008). LNA-mediated microRNA silencing in non-human primates. Nature *452*, 896–899.

Eulalio, A., Huntzinger, E., Nishihara, T., Rehwinkel, J., Fauser, M., and Izaurralde, E. (2009). Deadenylation is a widespread effect of miRNA regulation. RNA *15*, 21–32.

Grady, W.M., Parkin, R.K., Mitchell, P.S., Lee, J.H., Kim, Y.H., Tsuchiya, K.D., Washington, M.K., Paraskeva, C., Willson, J.K., Kaz, A.M., et al. (2008). Epigenetic silencing of the intronic microRNA hsa-miR-342 and its host gene EVL in colorectal cancer. Oncogene *27*, 3880–3888.

Hébert, S.S., Horré, K., Nicolaï, L., Papadopoulou, A.S., Mandemakers, W., Silahtaroglu, A.N., Kauppinen, S., Delacourte, A., and De Strooper, B. (2008). Loss of microRNA cluster miR-29a/b-1 in sporadic Alzheimer's disease correlates with increased BACE1/beta-secretase expression. Proc. Natl. Acad. Sci. USA *105*, 6415–6420.

Hedstrom, K.L., Ogawa, Y., and Rasband, M.N. (2008). AnkyrinG is required for maintenance of the axon initial segment and neuronal polarity. J. Cell Biol. *183*, 635–640.

Hollander, J.A., Im, H.I., Amelio, A.L., Kocerha, J., Bali, P., Lu, Q., Willoughby, D., Wahlestedt, C., Conkright, M.D., and Kenny, P.J. (2010). Striatal microRNA controls cocaine intake through CREB signalling. Nature *466*, 197–202.

Jin, P., Zarnescu, D.C., Ceman, S., Nakamoto, M., Mowrey, J., Jongens, T.A., Nelson, D.L., Moses, K., and Warren, S.T. (2004). Biochemical and genetic interaction between the fragile X mental retardation protein and the microRNA pathway. Nat. Neurosci. *7*, 113–117.

Kapfhamer, D., Miller, D.E., Lambert, S., Bennett, V., Glover, T.W., and Burmeister, M. (1995). Chromosomal localization of the ankyrinG gene (ANK3/Ank3) to human 10q21 and mouse 10. Genomics *27*, 189–191.

Kordeli, E., Lambert, S., and Bennett, V. (1995). AnkyrinG. A new ankyrin gene with neural-specific isoforms localized at the axonal initial segment and node of Ranvier. J. Biol. Chem. *270*, 2352–2359.

Krichevsky, A.M., King, K.S., Donahue, C.P., Khrapko, K., and Kosik, K.S. (2003). A microRNA array reveals extensive regulation of microRNAs during brain development. RNA *9*, 1274–1281.

Lagos-Quintana, M., Rauhut, R., Lendeckel, W., and Tuschl, T. (2001). Identification of novel genes coding for small expressed RNAs. Science *294*, 853–858.

Lazarov, O., Morfini, G.A., Pigino, G., Gadadhar, A., Chen, X., Robinson, J., Ho, H., Brady, S.T., and Sisodia, S.S. (2007). Impairments in fast axonal transport and motor neuron deficits in transgenic mice expressing familial Alzheimer's disease-linked mutant presenilin 1. J. Neurosci. *27*, 7011–7020.

Li, Y.Y., Cui, J.G., Hill, J.M., Bhattacharjee, S., Zhao, Y., and Lukiw, W.J. (2011). Increased expression of miRNA-146a in Alzheimer's disease transgenic mouse models. Neurosci. Lett. *487*, 94–98.

Lukiw, W.J. (2007). Micro-RNA speciation in fetal, adult and Alzheimer's disease hippocampus. Neuroreport *18*, 297–300.

Lukiw, W.J., Zhao, Y., and Cui, J.G. (2008). An NF-kappaB-sensitive micro RNA-146a-mediated inflammatory circuit in Alzheimer disease and in stressed human brain cells. J. Biol. Chem. *283*, 31315–31322.

Meister, G. (2007). miRNAs get an early start on translational silencing. Cell *131*, 25–28.

Nelson, P.T., and Wang, W.X. (2010). MiR-107 is reduced in Alzheimer's disease brain neocortex: validation study. J. Alzheimers Dis. *21*, 75–79.

Nunez-Iglesias, J., Liu, C.C., Morgan, T.E., Finch, C.E., and Zhou, X.J. (2010). Joint genome-wide profiling of miRNA and mRNA expression in Alzheimer's disease cortex reveals altered miRNA regulation. PLoS ONE *5*, e8898.

Pan, Z., Kao, T., Horvath, Z., Lemos, J., Sul, J.Y., Cranstoun, S.D., Bennett, V., Scherer, S.S., and Cooper, E.C. (2006). A common ankyrin-G-based mechanism retains KCNQ and NaV channels at electrically active domains of the axon. J. Neurosci. *26*, 2599–2613.

Peters, L., and Meister, G. (2007). Argonaute proteins: mediators of RNA silencing. Mol. Cell *26*, 611–623.

Price, D.L., Sisodia, S.S., and Gandy, S.E. (1995). Amyloid beta amyloidosis in Alzheimer's disease. Curr. Opin. Neurol. *8*, 268–274.

Rasband, M.N. (2010). The axon initial segment and the maintenance of neuronal polarity. Nat. Rev. Neurosci. *11*, 552–562.

Roy, S., Zhang, B., Lee, V.M., and Trojanowski, J.Q. (2005). Axonal transport defects: a common theme in neurodegenerative diseases. Acta Neuropathol. *109*, 5–13.

Schafer, D.P., Jha, S., Liu, F., Akella, T., McCullough, L.D., and Rasband, M.N. (2009). Disruption of the axon initial segment cytoskeleton is a new mechanism for neuronal injury. J. Neurosci. *29*, 13242–13254.

Schipper, H.M., Maes, O.C., Chertkow, H.M., and Wang, E. (2007). MicroRNA expression in Alzheimer blood mononuclear cells. Gene Regul Syst Bio *1*, 263–274.

Seitz, V., Butzhammer, P., Hirsch, B., Hecht, J., Gütgemann, I., Ehlers, A., Lenze, D., Oker, E., Sommerfeld, A., von der Wall, E., et al. (2011). Deep sequencing of MYC DNA-binding sites in Burkitt lymphoma. PLoS ONE *6*, e26837.

Selbach, M., Schwanhäusser, B., Thierfelder, N., Fang, Z., Khanin, R., and Rajewsky, N. (2008). Widespread changes in protein synthesis induced by microRNAs. Nature *455*, 58–63.

Shioya, M., Obayashi, S., Tabunoki, H., Arima, K., Saito, Y., Ishida, T., and Satoh, J. (2010). Aberrant microRNA expression in the brains of neurodegenerative diseases: miR-29a decreased in Alzheimer disease brains targets neurone navigator 3. Neuropathol. Appl. Neurobiol. *36*, 320–330.

Smalley, M.J., and Dale, T.C. (1999). Wnt signalling in mammalian development and cancer. Cancer Metastasis Rev. *18*, 215–230.

Sobotzik, J.M., Sie, J.M., Politi, C., Del Turco, D., Bennett, V., Deller, T., and Schultz, C. (2009). AnkyrinG is required to maintain axo-dendritic polarity in vivo. Proc. Natl. Acad. Sci. USA *106*, 17564–17569.

Song, A.H., Wang, D., Chen, G., Li, Y., Luo, J., Duan, S., and Poo, M.M. (2009). A selective filter for cytoplasmic transport at the axon initial segment. Cell *136*, 1148–1160.

Soriano, S., Kang, D.E., Fu, M., Pestell, R., Chevallier, N., Zheng, H., and Koo, E.H. (2001). Presenilin 1 negatively regulates beta-catenin/T cell factor/lymphoid enhancer factor-1 signaling independently of beta-amyloid precursor protein and notch processing. J. Cell Biol. *152*, 785–794.

Szu-Yu Ho, T., and Rasband, M.N. (2011). Maintenance of neuronal polarity. Dev. Neurobiol. *71*, 474–482.

Wang, W.X., Rajeev, B.W., Stromberg, A.J., Ren, N., Tang, G., Huang, Q., Rigoutsos, I., and Nelson, P.T. (2008). The expression of microRNA miR-107 decreases early in Alzheimer's disease and may accelerate disease progression through regulation of beta-site amyloid precursor protein-cleaving enzyme 1. J. Neurosci. *28*, 1213–1223.

Wang, X., Liu, P., Zhu, H., Xu, Y., Ma, C., Dai, X., Huang, L., Liu, Y., Zhang, L., and Qin, C. (2009). miR-34a, a microRNA up-regulated in a double transgenic mouse model of Alzheimer's disease, inhibits bcl2 translation. Brain Res. Bull. *80*, 268–273.

Westholm, J.O., and Lai, E.C. (2011). Mirtrons: microRNA biogenesis via splicing. Biochimie *93*, 1897–1904.

Wirths, O., Weis, J., Szczygielski, J., Multhaup, G., and Bayer, T.A. (2006). Axonopathy in an APP/PS1 transgenic mouse model of Alzheimer's disease. Acta Neuropathol. *111*, 312–319.

Yagishita, S. (1978). Morphological investigations on axonal swellings and spheroids in various human diseases. Virchows Arch. A Pathol. Anat. Histol. *378*, 181–197.

Yao, J., Hennessey, T., Flynt, A., Lai, E., Beal, M.F., and Lin, M.T. (2010). MicroRNA-related cofilin abnormality in Alzheimer's disease. PLoS ONE *5*, e15546.